PROCEEDINGS OF SCIENCE

Indications for BSM from unification, vacuum stability and gravitational waves

Kamila Kowalska,[a,*] **Dinesh Kumar,**[b] **Daniele Rizzo**[a] **and Enrico Maria Sessolo**[a]

[a] *National Centre for Nuclear Research, Pasteura 7, 02-093 Warsaw, Poland*

[b] *Department of Physics, University of Rajasthan, Jaipur 302004, India*

E-mail: Kamila.Kowalska@ncbj.gov.pl, dineshsuman09@gmail.com, Daniele.Rizzo@ncbj.gov.pl, Enrico.Sessolo@ncbj.gov.pl

We present a comprehensive list of the Standard Model extensions with vector-like fermions that allow precise unification of the Standard Model gauge couplings. The upper limits on vector-like masses from proton decay measurements are derived. At the same time, the presence of colored vector-like fermions in the spectrum stabilizes the electroweak vacuum if no Yukawa interactions are present. If this is not the case, vacuum stability may impose an upper bound on the allowed size of the Yukawa couplings. Finally, we consider a scenario in which the precise unification models are extended by an extra gauge $U(1)_X$ symmetry spontaneously broken by a Standard Model singlet scalar field. We show that an accompanying signal in the gravitational wave interferometers can discriminate between various unification scenarios.

Proceedings of the Corfu Summer Institute 2024 "School and Workshops on Elementary Particle Physics and Gravity" (CORFU2024) 12 - 26 May, and 25 August - 27 September, 2024
Corfu, Greece

*Speaker

 ISSN 1824-8039 . Published by SISSA Medialab.

PoS(CORFU2024)138

Contents

1. Introduction

Since the mid 1970s theorists have explored the enticing idea of unification of three fundamental forces of the Standard Model (SM) into a single gauge interaction [1–5]. While the very concept of unification as an underlying organizing principle stems to some extent from a sense of aesthetics, it finds a more robust justification in the fact that the renormalized gauge couplings of the SM, while evaluated at higher and higher energies, seem to converge towards a common value. This behavior might be understood as a manifestation of a new, unified description of fundamental interactions known as Grand Unified Theory (GUT).

Precise gauge coupling unification is not really achieved in the SM as discrepancies among the GUT-scale values of the SM couplings reach several percent. To make it work, the particle spectrum needs to be extended in order to modify the renormalization group (RG) running of the couplings below the GUT scale.[1] Supersymmetry (SUSY) has the advantage of leading quite naturally to gauge unification, yet no experimental evidence of low-scale SUSY has been found so far. While this fact does not undercut it completely as a theoretical framework, it is timely to ask to what extent unification of the gauge couplings is a unique property among various extensions of the SM. In other words, how many different beyond-the-SM (BSM) scenarios can be found whose particle spectrum differ quantitatively from the one of SUSY, and still allow for precise unification.

In Ref. [11] some of us addressed this question in a class of anomaly-free SM extensions featuring vector-like (VL) fermions,[2] which transform in two distinct representations under the group $SU(3)_c \times SU(2)_L \times U(1)_Y$ (we required that the SM gauge symmetry persists up to the unification scale). We analyzed all their possible combinations with the number of fermions in each representation limited only by perturbativity of the gauge couplings at the unification scale. We

[1] In principle, the GUT-scale values of the couplings can also be modified by high-scale threshold corrections [6–9]. These corrections, however, are strongly model dependent and for a certain range of the GUT-particle masses they become negligibly small [10]. Therefore, we neglect the effects of GUT threshold corrections throughout this study.

[2] BSM extension with scalars were discussed in [12].

identified 13 different combinations of two representations that allow for precise gauge unification at energies higher than 10^{15} GeV, with the VL masses in the range 0.25 – 10 TeV.[3] We also discussed a variety of experimental methods that allow one to test successful unification scenarios, including proton decay measurements, running of the strong gauge coupling, heavy stable charged particle (HSCP) searches, and electroweak (EW) precision tests. We demonstrated that by combining independent experimental results we manage in many cases to probe (and to exclude) essentially the whole parameter space of a given model.

In this proceedings we first review the results of Ref. [11] and present a comprehensive list of representations that allow for unification of the SM gauge couplings. We also mention experimental bounds that constrain the parameter space of the successful scenarios. We then report some recent results regarding the impact of VL fermions on the electroweak vacuum stability and their possible signatures in gravitational waves (GWs).

2. Unification with vector-like fermions

We first construct a set of generic extensions of the SM that satisfy the requirements defined in the introduction, i.e. no extra gauge symmetry is imposed, the only new particles in the spectrum are VL fermions, and the renormalized couplings remain perturbative at the unification scale. We additionally assume for the purpose of this study that any Yukawa interactions generated by the BSM sector and allowed by the gauge symmetry are negligible. We thus introduce N_{F_i} copies of new fermionic fields, which transform under the $SU(3)_c \times SU(2)_L \times U(1)_Y$ gauge group as VL multiplets

$$(R_{3F_i}, R_{2F_i}, Y_{F_i}) \oplus (\bar{R}_{3F_i}, \bar{R}_{2F_i}, -Y_{F_i}). \tag{1}$$

Note that we count separately over both components of the pair, so N_{F_i} can only assume even values (with an exception of fermions that transform in an adjoint representation of a non-abelian gauge symmetry group). The index i runs over the number of distinct representations. The upper bounds on dimension of possible VL representations and on the number of fermions that transform accordingly are provided by the perturbativity condition.

We further assume that at the unification scale the $SU(5)$ symmetry is restored and VL fermions are embedded into multiplets of $SU(5)$ just like it is the case for the SM fields. Taking into account the perturbativity bounds, there are 24 distinct non-singlet $SU(3)_c \times SU(2)_L \times U(1)_Y$ representations to consider:

$$\begin{aligned}
\text{color singlets}: \quad & (\mathbf{1},\mathbf{1},1)\,,\ (\mathbf{1},\mathbf{1},-2)\,,\ \left(\mathbf{1},\mathbf{2},\tfrac{1}{2}\right),\ \left(\mathbf{1},\mathbf{2},-\tfrac{3}{2}\right),\ (\mathbf{1},\mathbf{3},0)\,,\ (\mathbf{1},\mathbf{3},1)\,, \\
& \left(\mathbf{1},\mathbf{4},\tfrac{1}{2}\right),\ \left(\mathbf{1},\mathbf{4},-\tfrac{3}{2}\right), \\
\text{color triplets}: \quad & \left(\mathbf{3},\mathbf{1},-\tfrac{1}{3}\right),\ \left(\bar{\mathbf{3}},\mathbf{1},-\tfrac{2}{3}\right),\ \left(\bar{\mathbf{3}},\mathbf{1},\tfrac{4}{3}\right),\ \left(\bar{\mathbf{3}},\mathbf{1},-\tfrac{5}{3}\right),\ \left(\mathbf{3},\mathbf{2},\tfrac{1}{6}\right),\ \left(\bar{\mathbf{3}},\mathbf{2},\tfrac{5}{6}\right), \\
& \left(\bar{\mathbf{3}},\mathbf{2},-\tfrac{7}{6}\right),\ \left(\mathbf{3},\mathbf{3},-\tfrac{1}{3}\right),\ \left(\bar{\mathbf{3}},\mathbf{3},-\tfrac{2}{3}\right), \\
\text{color sextets}: \quad & \left(\bar{\mathbf{6}},\mathbf{1},-\tfrac{1}{3}\right),\ \left(\mathbf{6},\mathbf{1},-\tfrac{2}{3}\right),\ \left(\bar{\mathbf{6}},\mathbf{2},\tfrac{1}{6}\right),\ \left(\mathbf{6},\mathbf{2},\tfrac{5}{6}\right), \\
\text{color octets}: \quad & (\mathbf{8},\mathbf{1},0)\,,\ (\mathbf{8},\mathbf{1},1)\,,\ \left(\mathbf{8},\mathbf{2},\tfrac{1}{2}\right).
\end{aligned} \tag{2}$$

[3] Our results confirm and extend the findings of Ref. [13].

Using the representations of Eq. 2 as building blocks, we look for all the SM extensions with two distinct VL fermion types that could potentially lead to precise unification of three SM gauge couplings at the energies in the range $[10^{15} - 10^{18}]$ GeV. We run the SM gauge couplings from the low-energy scale, which we identify with the top quark mass M_t and at which the couplings assume the following values [14]

$$g_3(M_t) = 1.16660\,, \qquad g_2(M_t) = 0.64779\,, \qquad g_Y(M_t) = 0.35830\,. \tag{3}$$

We use the 2-loop SM RGEs from M_t up to the scale M_1, at which the lightest of VL fermions show up in the spectrum. We assume for simplicity that all N_F copies of the same representation have a common mass. Above M_1 we switch to the 2-loop RGEs for a generic BSM scenario, which can be found in Appendix A of Ref. [11]. At the scale M_2 the effects of heavier VL fermions need to be taken into account. Finally, we define a unification scale, $M_{\rm GUT}$, as the scale at which all three gauge couplings acquire a common value, $g_{M_{\rm GUT}} = g_3(M_{\rm GUT}) = g_2(M_{\rm GUT}) = g_1(M_{\rm GUT})$. We also require that the unified coupling is perturbative, i.e. $g_{M_{\rm GUT}} \leq 4\pi$.

We quantify the precision of the gauge coupling unification by a set of three mismatch parameters, $\epsilon_{1,2,3}$. For each combinations (i, j), where $i, j = 1, 2, 3$, we determine a two coupling unification scale from the condition $g_i(M^{ij}_{\rm GUT}) = g_j(M^{ij}_{\rm GUT}) = g_{ij}$. We then define a deviation of the third coupling from g_{ij} as

$$\epsilon_k = \frac{g_k^2(M^{ij}_{\rm GUT}) - g_{ij}^2}{g_{ij}^2} \tag{4}$$

and determine the true unification scale by requiring $\epsilon_{\rm GUT} = \min(\epsilon_1, \epsilon_2, \epsilon_3)$. In the SM $\epsilon^{\rm SM}_{\rm GUT} = 7.3\%$, while in the minimal SUSY version of the SM $\epsilon^{\rm MSSM}_{\rm GUT} = 1.1\%$ when all sparticle masses set at 1 TeV. Therefore, we define the precise gauge unification (PGU) by a condition $\epsilon \leq 1\%$.

For each of 276 scenarios with two distinctive VL representations we scan over the number of BSM fermions, N_1, N_2, and their masses, M_1, M_2, and for each point in the 4-dimensional parameter space we determine $\epsilon_{\rm GUT}$ and $M_{\rm GUT}$. The parameters M_1 and M_2 are varied between 0.25 TeV and 10 TeV. The main results of the analyses are summarized in Table 1. We found 13 different scenarios that allow for the PGU at the scale $10^{15} - 10^{18}$ GeV.

Whether the gauge coupling unification is possible in a given model hinges strongly on the hierarchy among the VL fermion masses. To illustrate this dependence, in Fig. 1 we present a distribution of the mismatch parameter $\epsilon_{\rm GUT}$ as a function of M_1 and M_2 for models F1 (left), F3 (center) and F13 (right). In red the region of the PGU is indicated. There are two main features that differentiate the phenomenological properties of the successful PGU scenarios. One is the mass hierarchy among the VL fermions: i) $M_1 \sim M_2$ (F1, F3, F4), ii) $M_1 \gg M_2$ (F6, F8, F9, F11, F12), and iii) $M_1 \ll M_2$ (F2, F5, F7, F10, F13). The other is the magnitude of the unification scale: i) $M_{\rm GUT} \simeq 10^{15}$ GeV (F1, F4, F9), ii) $M_{\rm GUT} \simeq 10^{16}$ GeV (F2, F5, F6, F7, F10, F11, F12), and iii) $M_{\rm GUT} \simeq 10^{17}$ GeV (F3, F8, F13). These two properties determine the experimental strategy for probing the allowed parameter space of a given model.

In particular, null results from the proton decay experiments offer an effective and model independent way of testing the PGU scenarios. Proton decay is a generic prediction of grand unification. The strongest lower bound on the proton lifetime is set by Super-Kamiokande (SK) underground water Cherenkov detector in the decay channel $p \to e^+\pi^0$ and reads $\tau_p > 1.6 \times 10^{34}$

Scenario	$\mathbf{R_{F_1}}$	$\mathbf{R_{F_2}}$	N_1	N_2
F1	$\left(\mathbf{1},\mathbf{2},\frac{1}{2}\right)$	$\left(\mathbf{6},\mathbf{1},\frac{1}{3}\right)$	12	2
F2	$\left(\mathbf{1},\mathbf{2},\frac{1}{2}\right)$	$\left(\mathbf{6},\mathbf{1},\frac{1}{3}\right)$	20	4
F3	$\left(\mathbf{1},\mathbf{2},\frac{1}{2}\right)$	$\left(\mathbf{6},\mathbf{1},\frac{1}{3}\right)$	22	4
F4	$\left(\mathbf{1},\mathbf{2},\frac{1}{2}\right)$	$(\mathbf{8},\mathbf{1},0)$	8	1
F5	$\left(\mathbf{1},\mathbf{2},\frac{1}{2}\right)$	$(\mathbf{8},\mathbf{1},0)$	12	2
F6	$\left(\mathbf{1},\mathbf{2},\frac{1}{2}\right)$	$(\mathbf{8},\mathbf{1},0)$	14	2
F7	$(\mathbf{1},\mathbf{3},0)$	$\left(\mathbf{3},\mathbf{1},-\frac{1}{3}\right)$	2	8
F8	$(\mathbf{1},\mathbf{3},0)$	$\left(\mathbf{3},\mathbf{1},-\frac{1}{3}\right)$	3	12
F9	$(\mathbf{1},\mathbf{3},0)$	$\left(\mathbf{6},\mathbf{1},-\frac{2}{3}\right)$	3	2
F10	$\left(\mathbf{1},\mathbf{4},\frac{1}{2}\right)$	$\left(\mathbf{6},\mathbf{1},-\frac{2}{3}\right)$	2	4
F11	$\left(\mathbf{3},\mathbf{1},-\frac{1}{3}\right)$	$\left(\mathbf{3},\mathbf{2},\frac{1}{6}\right)$	2	2
F12	$\left(\mathbf{3},\mathbf{1},\frac{2}{3}\right)$	$\left(\mathbf{3},\mathbf{2},\frac{1}{6}\right)$	4	4
F13	$\left(\mathbf{3},\mathbf{1},\frac{2}{3}\right)$	$\left(\mathbf{3},\mathbf{2},\frac{1}{6}\right)$	6	6

Table 1: Scenarios with 2 representations of VL fermions that allow for the PGU ($\epsilon_{\rm GUT} \leq 1\%$) and the associated unification scale lies in the range $10^{15} - 10^{18}$ GeV. In columns 2 and 3 transformation properties of both representations with respect to the SM gauge symmetry group are given. Columns 4 and 5 display number of VL fermions in each representation.

years [15]. Hyper-Kamiokande (HK), a next-generation machine, will be able to extend the limit by at least one order of magnitude, up to $\sim 2 \times 10^{35}$ years [16]. Scenarios F1 and F4 are already entirely excluded by the SK measurements, while scenario F9 is going to be entirely tested by HK. Proton decay also provides a unique experimental way of testing the PGU scenarios characterized by a BSM sector at energy scales far above the reach of any present-day collider experiment. The resulting upper bounds on the allowed VL masses are reported in Table 2.

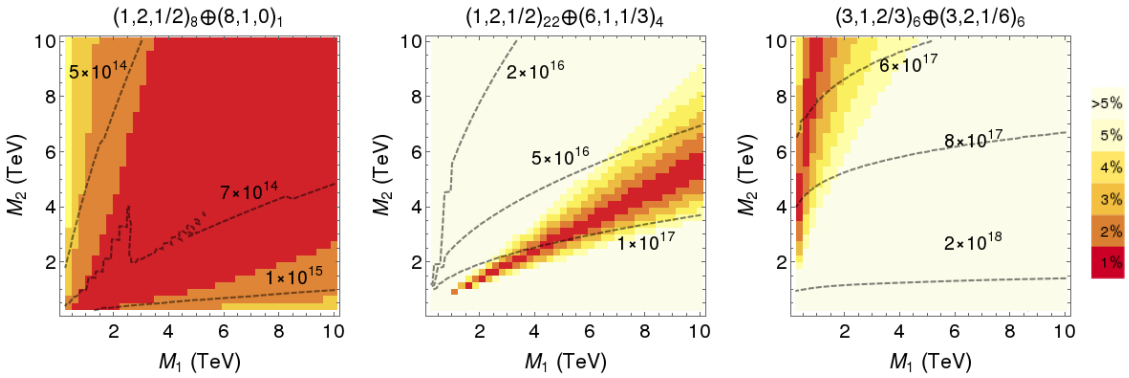

Figure 1: Distribution of the mismatch parameter $\epsilon_{\rm GUT}$ as a function of M_1 and M_2 for the scenarios F1 (left), F3 (center) and F13 (right). Red area corresponds to the PGU ($\epsilon_{\rm GUT} \leq 1\%$). Isocontours of the unification scale (in GeV) are indicated as dashed black curves.

Scenario	F2	F3	F5	F6	F7	F8	F10	F11	F12	F13
$M_1^{\max}$	25	350	10	500	20	2×10^5	250	600	6×10^4	-
$M_2^{\max}$	180	200	50	50	100	5×10^5	10^3	200	400	2×10^6

Table 2: Upper bounds on the VL masses M_1 and M_2 (in TeV) provided by the projected Hyper-Kamiokande measurement of the proton decay.

3. Constraints from vacuum stability

In the previous section we identified a class of BSM models, which are consistent with the requirement of the precise unification of the three SM gauge couplings. We now discuss another parameter whose RG running up to the GUT scale has important phenomenological consequences: the quartic couplings of the SM scalar potential. It is a well known fact that in the SM the EW vacuum is metastable [17], signalized by λ turning negative at the energies of around 10^9 GeV. On the other hand, extra degrees of freedom below the GUT scale may affect the RG evolution of the quartic coupling and help to stabilize the vacuum (see, for example, [18]).

It is no different in the PGU scenarios. As long as no Yukawa interactions between the VL fermions and the SM particles are present, the running of λ is only affected indirectly. In the presence of fermions charged under $SU(3)_c$, the beta function of the strong gauge coupling is modified in the following way:

$$\beta(g_3) = \frac{g_3^3}{16\pi^2}\left(-7 + \frac{2}{3}N_F S_2(R_3) d(R_2)\right), \tag{5}$$

where $S_2(R_3)$ is a Dynkin index of an $SU(3)_c$ representation R_3 and $d(R_2)$ is a dimension of an $SU(2)_L$ representation R_2. Since the BSM contribution is always positive, the value of g_3 at any renormalization scale above M_t is *larger* than in the standalone SM. As a consequence, the corresponding top Yukawa coupling becomes *smaller* than in the SM, due to a large and negative contribution from g_3,

$$\beta(y_t) = \frac{y_t}{16\pi^2}\left(\frac{9}{2}y_t^2 - 8g_3^2 - \frac{9}{4}g_2^2 - \frac{17}{20}g_Y^2\right). \tag{6}$$

Therefore, the impact of y_t on the running of the Higgs quartic coupling is reduced,

$$\beta(\lambda) = \frac{1}{16\pi^2}\left(24\lambda^2 + 12\lambda y_t^2 - 6y_t^4 + f(g_Y, g_2, \lambda)\right), \tag{7}$$

allowing λ to stay positive over the entire energy range from M_t up to the GUT scale.

In Fig. 2 we illustrate the impact of VL fermions on vacuum stability in the PGU models F2 (left) and F7 (right). The red dashed line shows the running of λ in the SM. The solid lines indicate the corresponding running in the presence of VL fermions, with the VL masses set to their minimal values allowed by the collider experiments (blue), and to their maximal values allowed by the proton decay experiments (green), see Table 2. In general, two qualitatively different situations may arise. The mere presence of VL fermions in the spectrum stabilizes the vacuum, irrespectively of their mass, like it happens in model F2. Or - as it is in model F7 - the vacuum is stabilized only with the VL fermions which are light enough. In such a case, imposing the EW vacuum stability as a constraint on a given PGU model provides an additional model-independent upper bound on the VL masses, which is stronger than the bound from the proton decay.

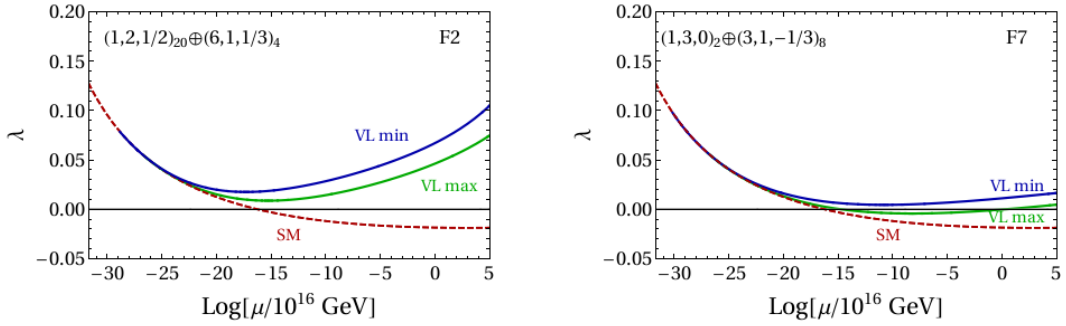

Figure 2: Running of the Higgs quartic coupling in the SM (red) and in the PGU models F2 (left) and F7 (right). The color code is explained in the text.

Let us now allow Yukawa interactions between the SM Higgs (denoted as h), SM fermions (denoted as q, d, u and e), and VL fermions of the PGU models (denoted as Q, D, U and L):

$$\begin{aligned}
\mathcal{L}_{F_2,F_3,F_5,F_6} &\supset -Y_{L,i}\, h^\dagger\, L_i\, e + \text{h.c.}\,, \\
\mathcal{L}_{F_7,F_8} &\supset -Y_{D,i}\, h^\dagger\, D_i\, q + \text{h.c.}\,, \\
\mathcal{L}_{F_{11}} &\supset -Y_{D,i}\, h^\dagger\, D_i\, q - Y_{Q_u,i}\, h\, Q_i\, u - Y_{Q_d,i}\, h^\dagger\, Q_i\, d - Y_4\, h^\dagger\, D\, Q - \tilde{Y}_4\, h\, D'\, Q' + \text{h.c.}\,, \\
\mathcal{L}_{F_{12,13}} &\supset -Y_{U,i}\, h\, U\, q_i - Y_{Q_u,i}\, h\, Q\, u_i - Y_{Q_d,i}\, h^\dagger\, Q\, d_i - Y_6\, h\, U\, Q - \tilde{Y}_6\, h\, U'\, Q' + \text{h.c.}\,.
\end{aligned} \tag{8}$$

These new Yukawa couplings generate additional contributions to the beta function of the SM quartic coupling,

$$\beta(\lambda) \supset C\lambda y_{\text{BSM}}^2 - A y_{\text{BSM}}^4\,, \tag{9}$$

with A and C being positive numerical coefficients. If a BSM Yukawa coupling is large enough, the second addend in Eq. 9 dominates and λ runs towards the negative values faster than in the SM. Hence, the presence of Yukawa interactions destabilizes the EW vacuum. Imposing vacuum stability as an extra condition on validity of the PGU models, an upper bound on the size of BSM Yukawa couplings can be derived. This is illustrated in Fig. 3, where we show values assumed by λ at various benchmark renormalization scales, $Q = M_{\text{GUT}}$ (solid), $Q = 7\times10^{13}$ GeV (dashed) and $Q = 3\times10^{9}$ GeV (dotted), as a function of the BSM Yukawa coupling at the scale corresponding to

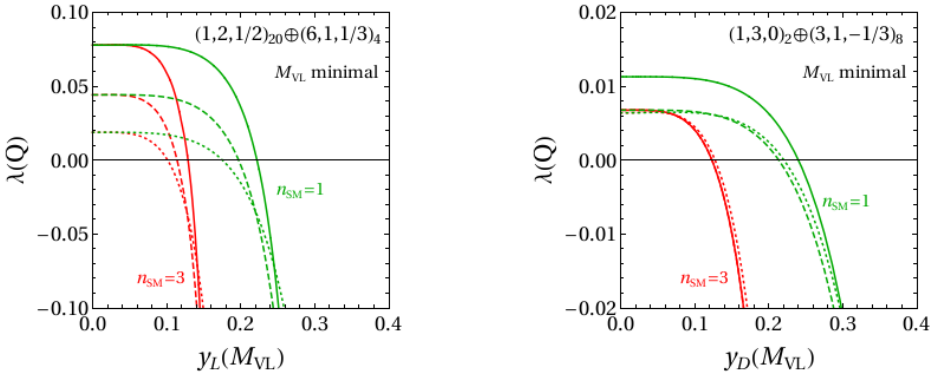

Figure 3: Running Higgs quartic coupling as a function of BSM Yukawa couplings in model F2 (left) and F7 (right). The color code is explained in the text.

the mass of a VL fermion participating in Yukawa interactions. Green color indicates VL fermions coupled to one generation of the SM quarks or leptons, while red refers to VL fermions coupled to all three SM families with the same strength. The upper bound on the BSM Yukawa couplings is to a large extent model independent, ranging from 0.1 to 0.3.

4. Signals in gravitational waves

In the previous section we discussed theoretical upper bounds on the size of Yukawa couplings in the PGU models, which may stem from imposing the requirement of the EW vacuum stability. Once the BSM Yukawa interactions with the SM Higgs are allowed, a natural question arises whether the SM scalar sector can be extended as well. Indeed, many GUT frameworks predict additional (light) scalars in the spectrum. For example, SM singlets may naturally emerge from the 24-dimensional adjoint representation of $SU(5)$. If a GUT symmetry is an $SU(N)$ with $N \geq 6$, two Higgs copies in fundamental representations are required in order to generate masses of up- and down-type quarks, leading to a 2HDM-like construction at low energies. Similarly, a symmetry breaking pattern $SU(6) \to SU(5) \times U(1)_X$ gives rise to an extra abelian gauge symmetry below the GUT scale and an accompanying SM singlet scalar to spontaneously break it. It is then interesting to investigate what could be complementary experimental signatures in the scalar sector.

There is a plethora of BSM scalar-dedicated searches at the colliders, in particular at the LHC. These are able to probe extended scalar sectors up to the energies of around TeV. In this study we focus instead on an enticing possibility to explore the BSM scalar sector through signals in GWs, generated by a first order phase transition (FOPT) in the early Universe. In the presence of a hot plasma, the effective scalar potential receives thermal corrections [19, 20], which generate a thermal barrier between the false and true vacua (cf. Appendix B of Ref. [21]). Tunneling from the former to the latter can proceed through bubble nucleation [22, 23], leading to the generation of GWs.

The GW physics is governed by several parameters that mainly depend on the shape of the effective thermal potential and on the bubbles' profile. These are the latent heat α, the nucleation speed β, and the reheating temperature $T_{\rm rh}$. We refer the reader to Appendix C of Ref. [21] for a brief review of the physics of FOPTs. The present-day GW signal is then characterized by the peak amplitude $\Omega^{\rm peak}(\alpha, \beta, T_{\rm rh})$ and the peak frequency $f^{\rm peak}(\alpha, \beta, T_{\rm rh})$,

$$h^2 \Omega_{\rm GW}(f) = h^2 \Omega^{\rm peak} \times \mathcal{F}(f/f^{\rm peak}) \,, \tag{10}$$

where $h = H_0/(100\,\mathrm{km/s/Mpc})$ is the present-day dimensionless Hubble parameter and $\mathcal{F}$ is a function of the frequency f. The explicit forms of the GW signal amplitudes are collected in Appendix C of Ref. [21].

Let us assume that the spectrum of the PGU models comprises an additional SM singlet scalar, S, charged under the U(1)$_X$ symmetry with $q_s = 2$. The tree-level scalar potential is then given by

$$V(H, S) = m_h^2\, h^\dagger g + m_S^2\, S^\dagger S + \lambda_1 \left(h^\dagger h\right)^2 + \lambda_2 \left(S^\dagger S\right)^2 + \lambda_3 \left(h^\dagger h\right)\left(S^\dagger S\right) \,. \tag{11}$$

It is enough to consider the effective potential for the radial component $\phi = \sqrt{2}\,\mathrm{Re}(S)$. The spontaneous breaking of $U(1)_X$ generates the mass of the abelian Z' gauge boson, which is approximately proportional to the vev along the S direction: $m_{Z'} \approx 2\, g_X v_S$. In such a setting the strength of the GW

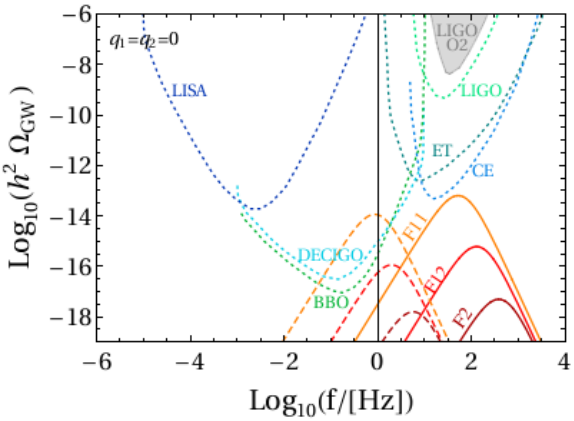

Figure 4: GW spectra for the scalar vev $v_S = 10^7$ GeV (solid) and $v_S = 10^5$ GeV (dashed) in the PGU scenarios F2, F11 and F12.

signal is determined by the size of the extra abelian gauge coupling (see [24–26] for early studies), with smaller values of g_X increasing supercooling and thus enhancing the signal's amplitude. In the presence of non-zero Yukwa interactions, Yukawa couplings tend to reduce the probability of tunneling from the false to true vacuum at a given temperature [21]. Additionally, in the framework of the PGU scenarios discussed in this study, the VL mass parameters M_1 and M_2 affect the shape of the thermal potential as well.

The requirement of the GUT-scale unification of the gauge coupling g_X with the three gauge couplings of the SM determines the running value of g_X at a renormalization scale Q as:

$$g_X^2(Q) = \frac{8\pi^2 g_{GUT}^2}{8\pi^2 + g_{GUT}^2\left[\frac{2}{3}d(R_{3_1})d(R_{2_1})N_1 q_1^2 + \frac{2}{3}d(R_{3_2})d(R_{2_2})N_2 q_2^2 + \frac{1}{3}q_S^2\right]\log(M_{GUT}/Q)}\,, \tag{12}$$

where q_1 and q_2 are the $U(1)_X$ charges of two VL fermion families, and N_1 and N_2 are their multiplicities. For example, assuming $q_1 = q_2 = 0$, one reads at $Q = 10^7$ GeV: $g_X(Q) = 0.84$ for F2, $g_X(Q) = 0.55$ for F11, and $g_X(Q) = 0.64$ for F12. Similarly, for $q_1 = q_2 = q_S$, we obtain at the same renormalization scale: $g_X(Q) = 0.14$ (F2), $g_X(Q) = 0.25$ (F11), and $g_X(Q) = 0.18$ (F12). Thus, in the absence of Yukawa interactions and an explicit scalar mass term m_S in the lagrangian, the GW signal corresponding to a given vev of S is entirely fixed by the unification condition. This is illustrated in Fig. 4, where we show the expected GW signals in the PGU scenarios F2, F11 and F12 for the benchmark vevs $v_S = 10^7$ GeV (solid) and $v_S = 10^5$ GeV (dashed). Superimposed are integrated sensitivity curves for the existing and planned space and ground interferometers. One can see that only scenario F11 (as well as scenario F7 characterized by a similar value of g_X) are in the reach of the GW experiments.

This conclusion strongly depends on the assumption regarding the $U(1)_X$ charges of VL fermions. If $q_1 = q_2 = q_S$, the renormalized g_X is too small to trigger a FOPT at the temperature above 1 GeV (at least for $v_S \lesssim 10^{13}$ GeV). To generate an observable GW signal, one would need to allow a small yet non-zero mass parameter m_S^2, along the lines of the discussion in Ref. [21].

Finally, one could consider a situation when only one of the two VL fermion representations is charged under the $U(1)_X$ symmetry group. In such a setting an interplay between the strength of

the GW signal and the size of the BSM Yukawa couplings can be investigated. This is going to be addressed in a forthcoming study [27].

5. Conclusions

In this proceedings we reported the results of several studies dedicated to BSM scenarios with VL fermions. Only a few models with two VL fermion representations allow for precise unification of the three SM gauge couplings, consistent with the bounds from perturbativity and proton life time. Interestingly, the latter can also provide model-independent upper bounds on VL masses. The presence of VL fermions in the spectrum can stabilize the EW vacuum. On the other hand, Yukawa couplings between the VL fermions and the SM particles have the opposite effect. As a result, an upper bound on the allowed strength of the BSM Yukawa interactions can be derived.

We also analyzed the possibility of observing GW signals in the scenarios where the SM scalar sector is extended by an S singlet field, which undergoes a FOPT. In the presence of an extra gauge symmetry factor $U(1)_X$ and under the assumption that VL fermions are $U(1)_X$ singlets, the strength of the signal is unambiguously determined by the unification condition.

References

[1] H. Georgi and S. L. Glashow, *Unity of All Elementary Particle Forces*, *Phys. Rev. Lett.* **32** (1974) 438–441.

[2] J. C. Pati and A. Salam, *Lepton Number as the Fourth Color*, *Phys. Rev.* **D10** (1974) 275–289. [Erratum: Phys. Rev.D11,703(1975)].

[3] R. N. Mohapatra and J. C. Pati, *Left-Right Gauge Symmetry and an Isoconjugate Model of CP Violation*, *Phys. Rev.* **D11** (1975) 566–571.

[4] H. Fritzsch and P. Minkowski, *Unified Interactions of Leptons and Hadrons*, *Annals Phys.* **93** (1975) 193–266.

[5] H. Georgi, *The State of the Art—Gauge Theories*, *AIP Conf. Proc.* **23** (1975) 575–582.

[6] G. P. Cook, K. T. Mahanthappa, and M. A. Sher, *Effects of Heavy Colored Higgs Scalars on SU(5) Predictions*, *Phys. Lett.* **90B** (1980) 398–400.

[7] V. V. Dixit and M. Sher, *The Futility of High Precision SO(10) Calculations*, *Phys. Rev.* **D40** (1989) 3765.

[8] P. Langacker and N. Polonsky, *Uncertainties in coupling constant unification*, *Phys. Rev.* **D47** (1993) 4028–4045, [hep-ph/9210235].

[9] K. Hagiwara and Y. Yamada, *Grand unification threshold effects in supersymmetric SU(5) models*, *Phys. Rev. Lett.* **70** (1993) 709–712.

[10] J. Schwichtenberg, *Gauge Coupling Unification without Supersymmetry*, *Eur. Phys. J.* **C79** (2019), no. 4 351, [arXiv:1808.10329].

[11] K. Kowalska and D. Kumar, *Road map through the desert: unification with vector-like fermions*, *JHEP* **12** (2019) 094, [arXiv:1910.00847].

[12] U. C. Olivas, K. Kowalska, and D. Kumar, *Road map through the desert with scalars*, *JHEP* **03** (2022) 132, [arXiv:2112.11742].

[13] B. Bhattacherjee, P. Byakti, A. Kushwaha, and S. K. Vempati, *Unification with Vector-like fermions and signals at LHC*, *JHEP* **05** (2018) 090, [arXiv:1702.06417].

[14] D. Buttazzo, G. Degrassi, P. P. Giardino, G. F. Giudice, F. Sala, A. Salvio, and A. Strumia, *Investigating the near-criticality of the Higgs boson*, *JHEP* **12** (2013) 089, [arXiv:1307.3536].

[15] **Super-Kamiokande** Collaboration, K. Abe et al., *Search for proton decay via $p \to e^+\pi^0$ and $p \to \mu^+\pi^0$ in 0.31 megaton·years exposure of the Super-Kamiokande water Cherenkov detector*, *Phys. Rev.* **D95** (2017), no. 1 012004, [arXiv:1610.03597].

[16] **Hyper-Kamiokande** Collaboration, K. Abe et al., *Hyper-Kamiokande Design Report*, arXiv:1805.04163.

[17] G. Degrassi, S. Di Vita, J. Elias-Miro, J. R. Espinosa, G. F. Giudice, G. Isidori, and A. Strumia, *Higgs mass and vacuum stability in the Standard Model at NNLO*, *JHEP* **08** (2012) 098, [arXiv:1205.6497].

[18] S. Gopalakrishna and A. Velusamy, *Higgs vacuum stability with vectorlike fermions*, *Phys. Rev. D* **99** (2019), no. 11 115020, [arXiv:1812.11303].

[19] S. Weinberg, *Gauge and global symmetries at high temperature*, *Phys. Rev. D* **9** (Jun, 1974) 3357–3378.

[20] L. Dolan and R. Jackiw, *Symmetry behavior at finite temperature*, *Phys. Rev. D* **9** (Jun, 1974) 3320–3341.

[21] A. Chikkaballi, K. Kowalska, and E. M. Sessolo, *Naturally small neutrino mass with asymptotic safety and gravitational-wave signatures*, *JHEP* **11** (2023) 224, [arXiv:2308.06114].

[22] A. Linde, *Fate of the false vacuum at finite temperature: Theory and applications*, *Physics Letters B* **100** (1981), no. 1 37–40.

[23] A. Linde, *Decay of the false vacuum at finite temperature*, *Nuclear Physics B* **216** (1983), no. 2 421–445.

[24] N. Okada and O. Seto, *Probing the seesaw scale with gravitational waves*, *Phys. Rev. D* **98** (2018), no. 6 063532, [arXiv:1807.00336].

[25] C. Marzo, L. Marzola, and V. Vaskonen, *Phase transition and vacuum stability in the classically conformal B–L model*, *Eur. Phys. J. C* **79** (2019), no. 7 601, [arXiv:1811.11169].

[26] J. Ellis, M. Lewicki, J. M. No, and V. Vaskonen, *Gravitational wave energy budget in strongly supercooled phase transitions*, *JCAP* **06** (2019) 024, [arXiv:1903.09642].

[27] K. Kowalska, D. Rizzo, and E. M. Sessolo. In preparation.